Fractalization of a torus as a strange nonchaotic attractor

Takashi Nishikawa* and Kunihiko Kaneko

Department of Pure and Applied Sciences, University of Tokyo, Komaba, Meguro-ku, Tokyo 153, Japan

(Received 1 July 1996)

Fractalization of a torus and its transition to chaos in a quasiperiodically forced logistic map is reinvestigated in relation to a strange nonchaotic attractor, with the aid of a functional equation for the invariant curve. The existence of a fractal torus in an interval in parameter space is confirmed by the length and the number of extrema of the torus attractor, as well as the Fourier mode analysis. Mechanisms of the onset of a fractal torus and the transition to chaos are studied in connection with the intermittency. [S1063-651X(96)07412-0]

PACS number(s): 05.45.+b

I. INTRODUCTION

The transition from a torus to chaos has been intensively investigated [1]. Two types of instabilities exist, which cause the collapse of tori: One is in the phase direction and the other in the amplitude direction. The former instability has already been studied in detail using the circle map, while the oscillation and fractalization of tori have been reported due to the instability in the amplitude direction. One of the authors (K.K.) reported that the oscillation of tori gets stronger with the increase of external forcing, until it reaches a fractal, and then chaos appears [2]. Although the fractal nature of the torus was confirmed at the onset of chaos, the strange oscillation of a torus before the onset remained unclear.

The existence of strange nonchaotic attractors (SNAs) was shown by Grebogi *et al.* [3]. Here the word ''strange'' refers to the geometry of the attractors and the word ''chaotic'' refers to the orbital instability of the dynamics. In a model with quasiperiodic forcing similar to that for the fractalization of a torus, they showed analytically that the attractor has a nonpositive Lyapunov exponent but a complicated geometry. Indeed, the attractor is not smooth on the set of dense points. Although the original model by Grebogi *et al.* [3] excludes the possibility of chaos, the SNA has generally been observed in a system where chaos appears with the increase of the forcing [4–10], as it was discussed in the fractalization of a torus [1,2].

In the present paper, we study how the transition from a smooth to a fractal torus occurs. We have confirmed that there is a parameter region with a nonzero measure where the SNA exists between the smooth torus and chaos. This leads to the following scenario of destruction of the tori: Torus →fractal torus (SNA)→chaos.

In the following sections, we will first characterize the nature of a fractal torus as a SNA. Besides the direct simulation of the quasiperiodically forced logistic map, we adopt the functional map to obtain the invariant torus. The length of the invariant curve, as well as the number of singular points, shows how the fractalization occurs with the parameter change. In Sec. III, a perturbation expansion of the functional equation is given, where the SNA is characterized by

the loss of the convergence in the Fourier mode expansion of the derivative of the invariant curve. A comparison between smooth and fractal tori is given in Sec. IV, where some dynamical signatures of the fractal torus are discussed, such as the parameter sensitivity of the Lyapunov exponent and the phase sensitivity. The onset of chaos from the SNA is investigated in Sec. V, where the transition is associated with the intermittency from the fixed point in the functional map.

II. FRACTALIZATION OF A TORUS AS A SNA

The transition from a torus to chaos has been studied with a variety of two-dimensional maps [1]. With the change of the bifurcation parameter, the amplitude of oscillation gets stronger, accompanied by phase lockings. To focus on the amplitude instability by excluding the phase locking, we choose the following two-dimensional map [2], with a constant rotation of the phase:

$$x_{n+1} = f(x_n) + \varepsilon g(\theta_n),$$

$$\theta_{n+1} = \theta_n + \omega \bmod 1. \tag{1}$$

Here x_n represents the amplitude, while θ_n corresponds to the phase of oscillation. To exclude the phase lockings no coupling from x to θ is included, where ω is an irrational number representing the rotation number.

In this paper we set $f(x) = ax(1-x)$, $g(\theta) = \sin 2\pi\theta$, and $\omega = (\sqrt{5}-1)/2$ as the simplest nonlinear map with an external driving force. For most simulations, we fix $a = 3.0$ and vary ε to see the change of the attractor. At $\varepsilon = 0$, the map, of course, is just a one-dimensional map of x_n with a fixed point $x^* = 1 - 1/a$. Thus the attractor of the two-dimensional map is just a straight-line torus. As ε is increased, oscillations of the torus start to appear, which become fractal with the dimension above one (as it is confirmed later by a direct measurement of the length of the torus). As ε is increased further, another transition from the fractal torus to chaos appears, by which the stability in the x direction is lost.

Three examples of the patterns of attractors are given in Fig. 1 corresponding to the three types of attractors, while the change of the Lyapunov exponent is plotted in Fig. 2. The transition from a torus to chaos occurs at $\varepsilon \sim 0.1573$. As it will be confirmed later, the torus loses its smoothness around $\varepsilon \sim 0.1553$. Hence the SNA exists in an interval of

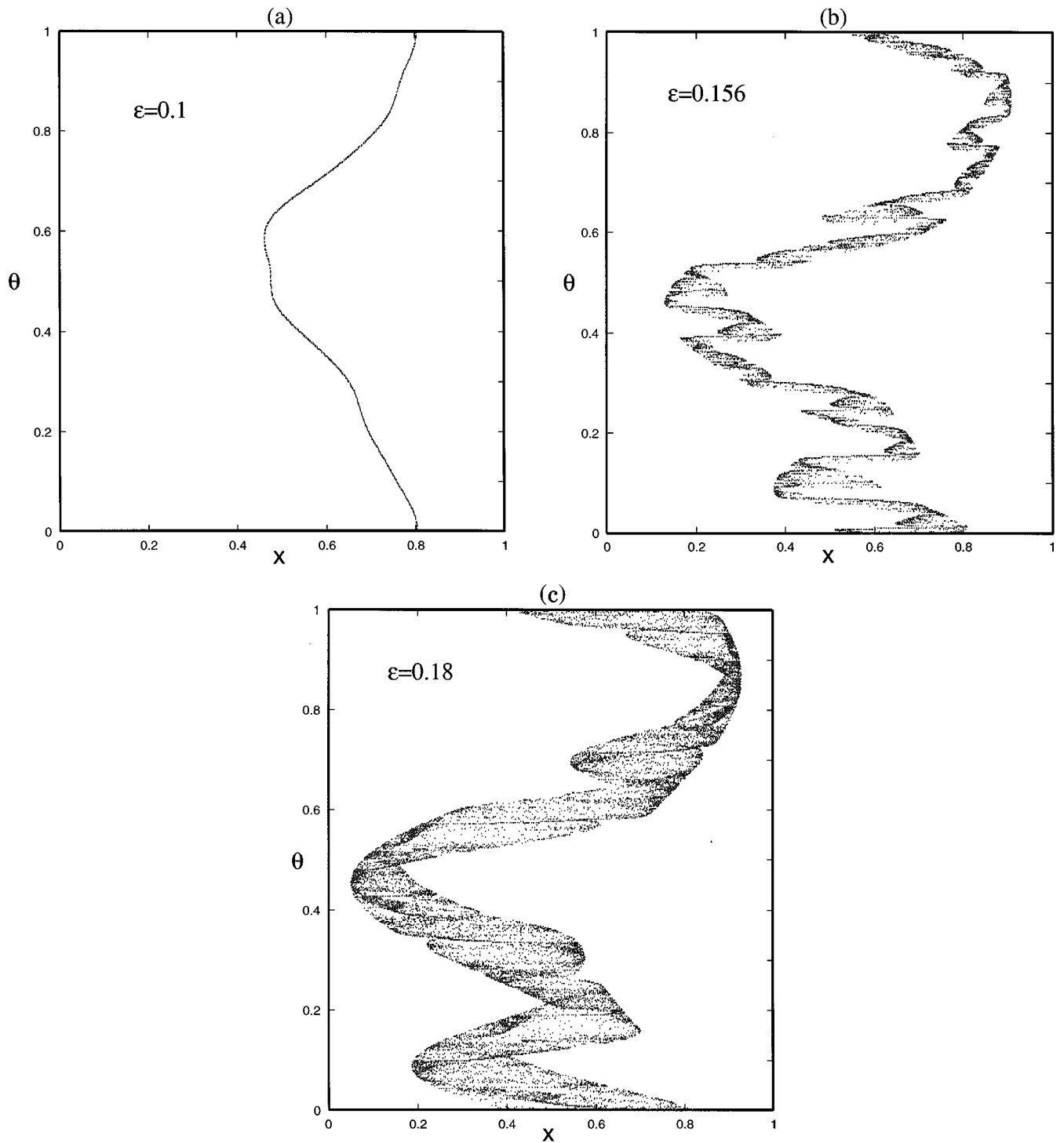*Present address: Deparment of Mathematics, University of Maryland at College Park, College Park, MD 20742.

FIG. 1. Three types of attractors. The value of ε in each figure is (a) $\varepsilon = 0.1$, (b) $\varepsilon = 0.156$, and (c) $\varepsilon = 0.18$, respectively. We have plotted 30 000 points after discarding initial transients, where $a = 3.0$ and $\omega = (\sqrt{5} - 1)/2$.

the parameter, where the Lyapunov exponent has a sharp sensitivity to ε, as in the chaotic region.

To confirm that the attractor has a noninteger dimension, we study the equation for the invariant torus, following the argument of [2]. In our model (1) the attractor is expressed as a single-valued function of θ, as $x = X(\theta)$ ($0 \leq \theta \leq 1$). If this function represents an invariant curve of the map, it must satisfy the functional equation

$$X(\theta + \omega; \text{mod} 1) = f(X(\theta)) + \varepsilon g(\theta)$$

$$= aX(\theta)[1 - X(\theta)] + \varepsilon \sin 2\pi\theta. \quad (2)$$

This equation is postulated by the constraint that the point (x_{n+1}, θ_{n+1}) should also be on the curve and is obtained by substituting x_n by $X(\theta)$ and x_{n+1} by $X(\theta + \omega)$ in the map
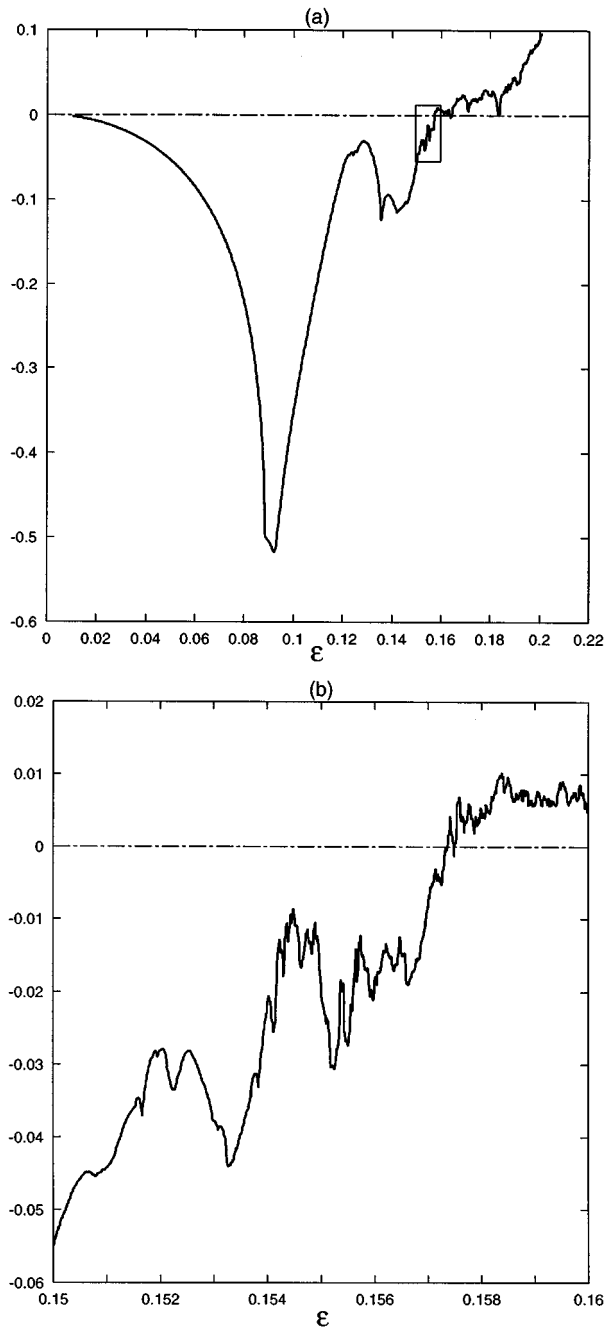
FIG. 2. Lyapunov exponents plotted versus the parameter ε. Computed from the average over 10^6 iterations of the map (1), after discarding initial 5000 points of transient.

(1). From this functional equation we can introduce the following "functional map," which maps one function to another function:

$$X_{n+1}(\theta+\omega;\text{mod}1)=f(X_n(\theta))+\varepsilon g(\theta)$$

$$=aX_n(\theta)[1-X_n(\theta)]+\varepsilon\sin2\pi\theta.$$

$$(3)$$

The attractor of the original map (1) is obtained as a fixed point in the *functional space*, for the iteration of the func-
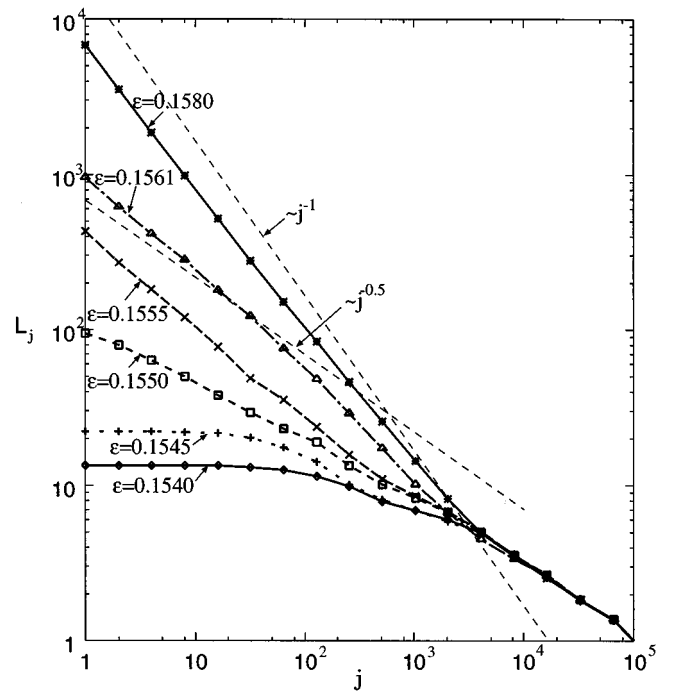

FIG. 3. Examples of a log-log plot of length versus mesh ($a=3.0$ and $F_k=317\,811$), obtained from the attractor of the functional map.

tional map (3). This discussion stands only if the Lyapunov exponent is negative and the attractor has a single value x for each θ.

Since the functional map (3) is an infinite-dimensional dynamical system, one cannot compute it directly. We have numerically computed it by approximating $\omega=(\sqrt{5}-1)/2$ by $\omega_k=F_{k-1}/F_k$, where $\{F_k\}_{k=0,1,\ldots}$ is a Fibonacci series. ($\omega_k\rightarrow\omega$ as $k\rightarrow\infty$.) This approximation transforms the functional map to an F_k-dimensional map that maps F_k lattice points on the θ coordinate onto themselves. We have computed the attractor of this F_k-dimensional map to obtain the approximate solution of the functional equation (2) as a piecewise-linear function.

For the parameter regime corresponding to the torus attractor, the convergence is rather fast. The convergence time of the functional map to a fixed point gets longer as ε approaches the onset of chaos, while for $\varepsilon>0.1573$, corresponding to the chaos region, the functional map does not converge to a fixed point.

The functional equation enables us to compute the length L_j of $X(\theta)$ as

$$L_j=\sum_{i=0}^{F_k-1}\sqrt{\left\{X\left(\frac{i}{F_k}\right)-X\left(\frac{i+j}{F_k}\right)\right\}^2+\left(\frac{j}{F_k}\right)^2}.\qquad(4)$$

If the dimension of the attractor is $1+\alpha$, L_j must scale as $L_j\propto j^{-\alpha}$, where $0<\alpha<1$. The slope of this plot α gives a kind of fractal dimension. Figure 3 is an example of the log-log plot of length L_j versus the mesh width j. Here we have adopted $F_k=317\,811$ for the approximation of ω.
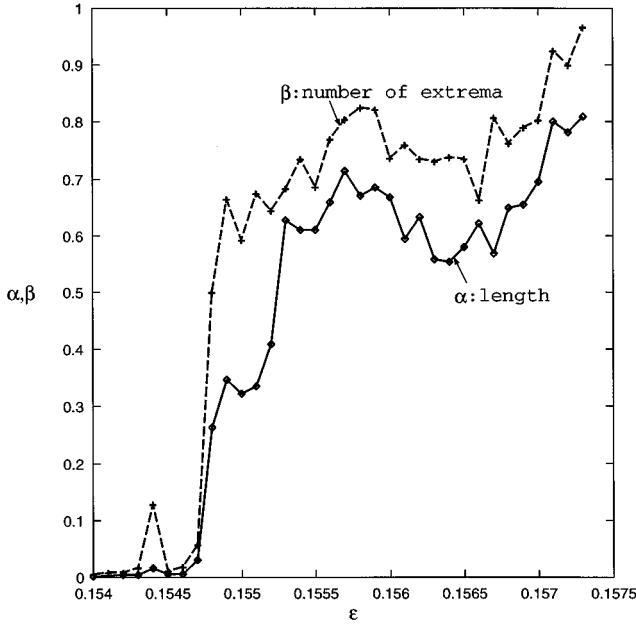
FIG. 4. Change of the slope α versus external forcing ε ($a=3.0$ and $F_k=317\,811$). The slope is estimated from the length at the five smallest mesh scales. The error bar is not explicitly given, but it is about 0.05 –0.1.

FIG. 5. Length of attractors with the mesh scale j. $F_k=9\,227\,465$ and $a=3.0$.

Hence $j=1$ corresponds to the mesh size of $1/317\,811\sim3\times10^{-6}$. Figure 4 is the plot of slope α versus external force ε.

The slope starts to be nonzero at the transition point at about $\varepsilon\sim0.1548$. The slope jumps to $\alpha\sim0.62$ and stays around the value with the increase of ε up to the vicinity of the onset of chaos.

In the region between $\varepsilon\approx0.1548$ and 0.1553, the exponent is roughly 0.3 up to fine mesh scales (e.g., $1/317\,811$), but there appears a saturation at a finer mesh. In Fig. 5 we have plotted the length versus mesh, taking $F_k=9\,227\,465$. There is a crossover to a smooth behavior at the scale about $10/9\,227\,465$ for $\varepsilon=0.1548$. Here we call this parameter regime a ''pre-fractal torus,'' since this region is distinguished from the smooth and fractal torus regimes. Indeed, the crossover to a smooth curve is seen only at a much finer scale than for a smooth-torus regime, while this crossover scale increases as ε approaches the onset parameter for the fractal torus. The slope at the scaling regime (i.e., scales with a larger mesh beyond the crossover) has a jump at the onset of the fractal torus: The exponent α in the scaling regime jumps from 0.3 to 0.62, when the parameter ε crosses 0.1553, the border between pre-fractal- and fractal-torus regimes.

For $\varepsilon>0.1573$, $X_n(\theta)$ does not converge to a fixed curve. Indeed, the Lyapunov exponent of the two-dimensional map is positive in this regime and the attractor here is chaotic. Summing up the results of the fractal exponent of Fig. 4 and the Lyapunov exponent of Fig. 2, one can conclude that the fractal torus exists at least in the region $0.1553<\varepsilon<0.1573$. (By numerical means, one cannot completely exclude the possibility that the fractal nature of the torus disappears as the mesh scale goes down to a much finer scale and the fractal torus exists only at the onset of chaos. Indeed, this suspicion has led to the report, in [2], of the
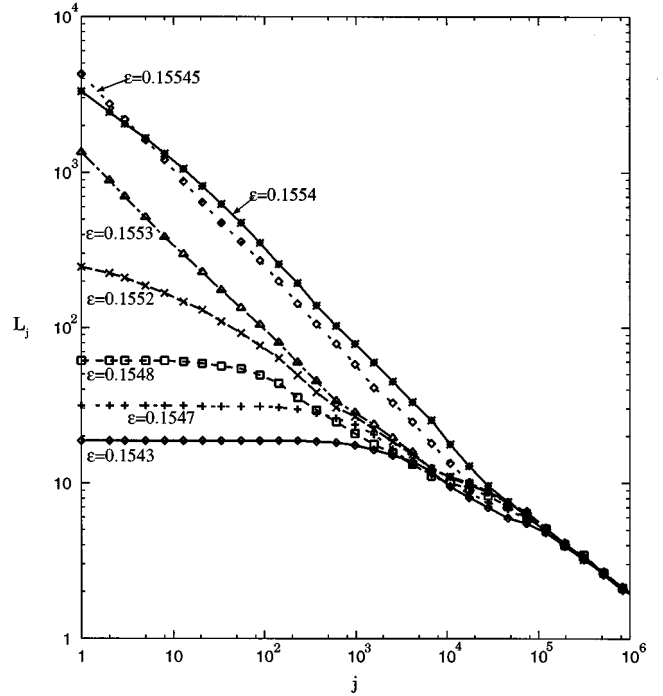
fractal torus only at a single parameter point. We assume that the scaling with the exponent α lasts to an infinitesimal scale since the increase of the crossover size near 0.1553 is so strong that it is distinguished from the pre-fractal-torus region.)

We have also measured the distribution of local dimensions, by varying ε, which is shown in Fig. 6. The distribution is single humped, with slight asymmetry. At the pre-fractal torus, the distribution has a peak around zero.

We have also calculated the number of extremal points of the function $X(\theta)$. Here the number N_j of extremal points for a given mesh is defined as follows. First count the number of the mesh point i such that

$$\left\{X\left(\frac{i+j}{F_k}\right)-X\left(\frac{i}{F_k}\right)\right\}\left\{X\left(\frac{i+2j}{F_k}\right)-X\left(\frac{i+j}{F_k}\right)\right\}<0 \quad (5)$$

is satisfied: Then N_j is obtained by dividing this number by j. Figure 7 gives some examples of the log-log plot of N_j versus j.

The number N_j increases as the mesh j is reduced, which means that the finer the mesh one uses, the more extrema appear. This is consistent with the fractal nature of the torus. However, we note that N_j scales not as $N_j\sim j^{-1}$ but as $N_j\sim j^{-\beta}$, where $0<\beta<1$. This means that the fraction of singular points decreases with the mesh. In other words, the extremal points lie on a Cantor set on the θ axis.

The dependence of β on the parameter ε is plotted in Fig. 4. The exponent stays around 0.75, while the fractal dimension stays around 0.6. Near the onset of chaos $\varepsilon=0.1573$, the exponent β increases, until it takes 1.0 at the onset. In other words, the ruggedness of the torus fills the space down to any small scale when the torus loses stability and is replaced by chaos.
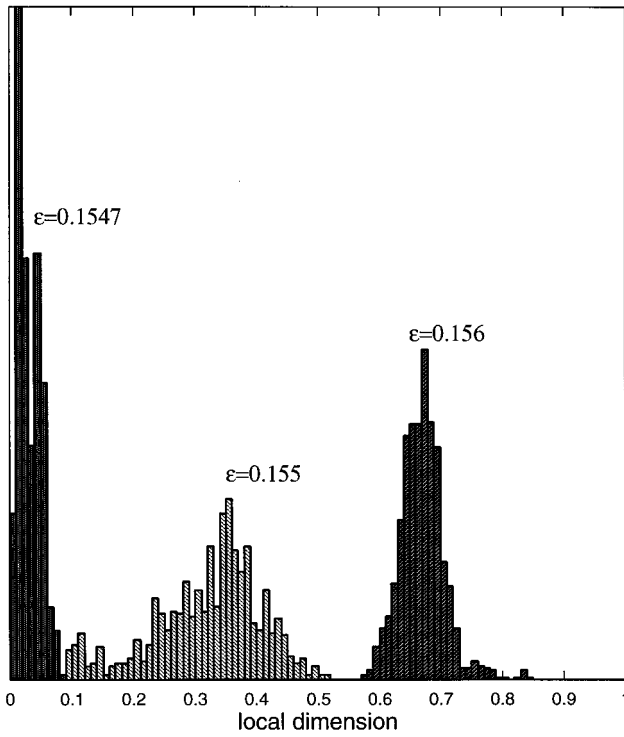
FIG. 6. Distribution of the local dimension obtained through the measurement of the local length. We have measured the length of $X(\theta)$ at each lattice point using 6000 lattice points around it. By computing the local dimension over all lattice points and sampling the number with the bin size 0.01, the distribution is obtained. ($a=3.0$.)
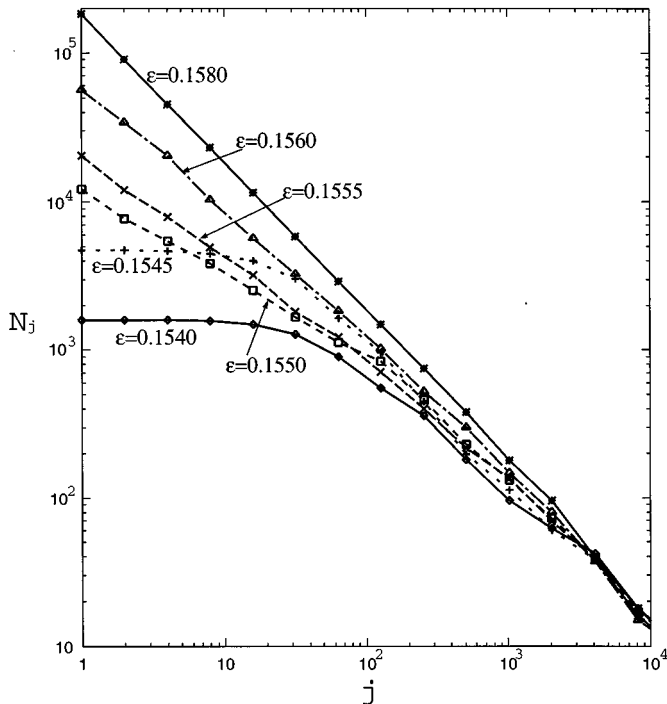

FIG. 7. Number of extremal points versus mesh size. See the text for the method of computation. ($a=3.0$ and $F_k=317\,811$.)
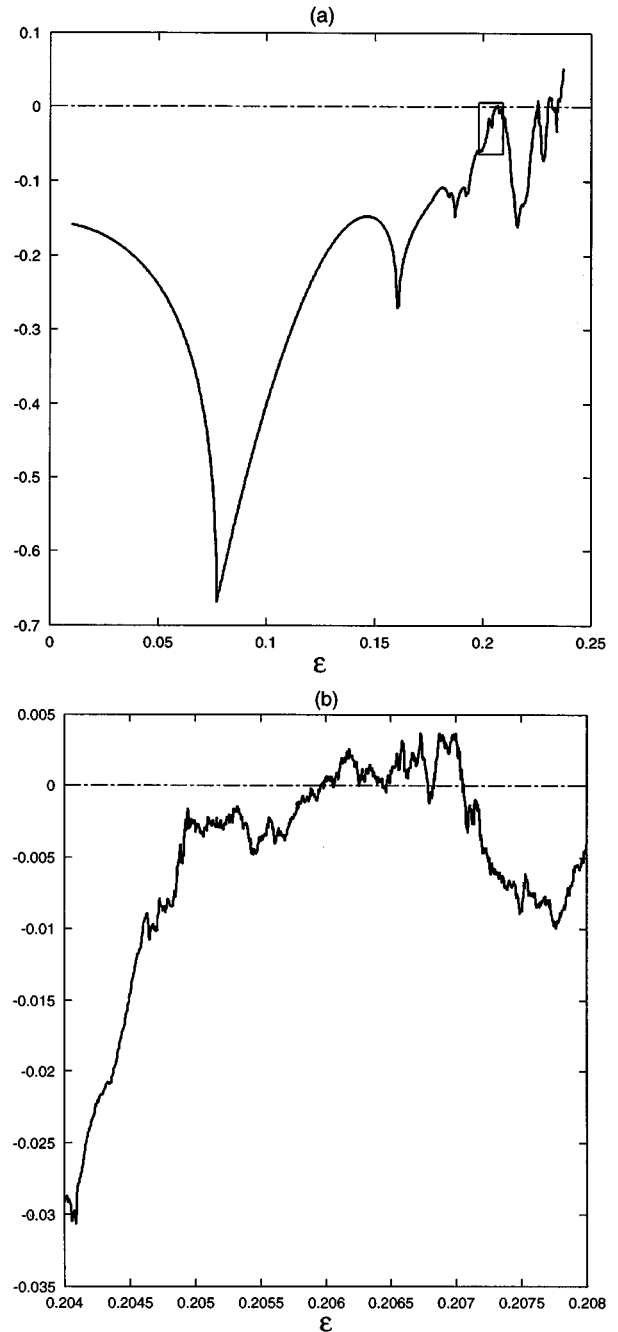

FIG. 8. (a) and (b) Change of the Lyapunov exponent with the parameter ε [$a=2.8$ and $\omega=(\sqrt{5}-1)/2$]. (b) is the blowup of (a) for $0.204<\varepsilon<0.208$. The exponent is computed from the average of 10^6 steps after discarding initial 5000 steps.

The linear increase of the extremum point agrees with the picture of a random curve. Consider, for example, a curve $C(i)$ (with i lattice point) generated by $C(i+1)=\delta C(i)+\eta$ with η a random number distributed over $[-1,1]$ and $\delta \le 1$. The number of extremum points increases linearly with the number of mesh points. The increase is given by $2N/3$ for $\delta=0$, while the increase is slower with a smaller proportional coefficient for $\delta>0$, until it is given by $N/2$ for $\delta=1$. Since the increase is given by $0.58N$ at the onset of chaotic (and also in the chaos region) in our simulation, the critical torus can be approximated by a
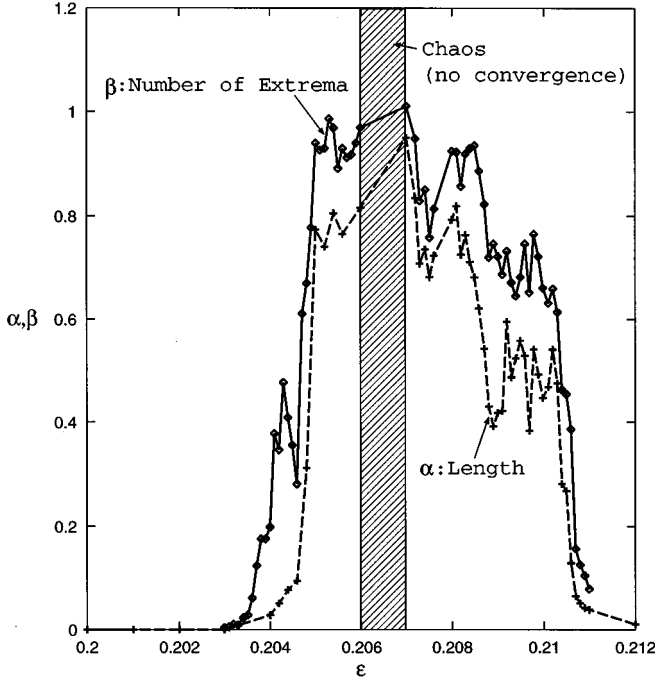
FIG. 9. Fractal dimension α (obtained by measuring the length) and the exponent β on the number of extremal points, plotted versus ε. Computed from the attractor of the functional map. ($a = 2.8$ and $F_k = 317\,811$.)

correlated random curve. This behavior and the coefficient characterize how the fractal torus collapses and is replaced by chaos in the two-dimensional map Eq. (1).

To close the present section, it is interesting to note the universality of our results. In the discovery of a fractal torus by [2], the parameter $a = -1$ was adopted, where successive transitions from a torus to a fractal torus and then to chaos was found with the increase of ε. We have reexamined the simulation using larger mesh sizes. Here again, a fractal torus exists for a finite interval of parameters, where the fractal dimension increases from 0.6 to about 0.88 with ε. The number of extremal points again increases with a fractional power, while it increases linearly at the onset of chaos.

Another interesting set of examples is given for $a = 2.8$. The Lyapunov exponent is plotted in Fig. 8, while the fractal dimension and the number of extremal points obtained from the functional equation (with the mesh 317 811) are given in Fig. 9.

From this figure one can see that windows of a fractal torus (FT) and a smooth torus (ST) appear beyond the onset of chaos. Indeed there are transition sequences among the ST, FT, and chaos, as seen in Figs. 8 and 9. At $\varepsilon \sim 0.204$ the FT appears, which is replaced by chaos at $\varepsilon \sim 0.206$. For

$\varepsilon \sim 0.207$, the ''inverse'' bifurcation from chaos to a FT and then to a ST (at $\varepsilon \sim 0.211$) proceeds. Further bifurcations to a FT and chaos and back to a ST are seen for larger ε. Again at the boundary between chaos and a fractal torus, the increase of the extremum points is almost linear.

III. FRACTAL TORUS VIEWED FROM A FUNCTIONAL MAP

In this section we apply the Fourier mode analysis to the functional equation (2). First we consider the Fourier expansion of $X(\theta)$,

$$X(\theta) = \sum_{k=-\infty}^{\infty} \hat{X}(k) e^{2\pi i k \theta}, \tag{6}$$

$$\hat{X}(k) = \int_0^1 X(\theta) e^{-2\pi i k \theta} d\theta, \tag{7}$$

and substitute it into (2). Then we have

$$\hat{X}(k) e^{2\pi i k \omega} = a\hat{X}(k) - a \sum_{k'=-\infty}^{\infty} \hat{X}(k')\hat{X}(k-k')$$

$$- \frac{i\varepsilon}{2}(\delta_{k,1} - \delta_{k,-1}). \tag{8}$$

Next we expand each Fourier mode $X(k)$ with respect to the powers of ε,

$$\hat{X}(k) = \sum_{n=0}^{\infty} \varepsilon^n \hat{X}_n(k). \tag{9}$$

Substituting this into (8) and comparing the terms of the same power of ε on both sides of the equation, we get

$$\hat{X}_n(k) e^{2\pi i k \omega} = a\hat{X}_n(k) - a \sum_{k'=-\infty}^{\infty} \sum_{m=0}^{n} \hat{X}_m(k')\hat{X}_{n-m}(k-k')$$

$$- \frac{i}{2}\delta_{n,1}(\delta_{k,1} - \delta_{k,-1}) \tag{10}$$

for each n. It is straightforward to show that $\hat{X}(k)$ has only terms ε^n such that $n \geq |k|$. This means that the term ε^n only has a Fourier mode with the wave number no more than n. The first three terms of $\hat{X}_n(k)$, $\hat{X}(k)$, and $X(\theta)$ are given as

$$\hat{X}_0(k) = \left(1 - \frac{1}{a}\right)\delta_{k,0}, \tag{11}$$

$$\hat{X}_1(k) = \frac{\pm i\delta_{k,\pm 1}}{2(e^{\pm 2\pi i \omega} + a - 2)}, \tag{12}$$

$$\hat{X}_2(k) = \frac{-a\{2\hat{X}_1(-1)\hat{X}_1(1)\delta_{k,0} + [\hat{X}_1(-1)]^2\delta_{k,-2} + [\hat{X}_1(1)]^2\delta_{k,2}\}}{e^{2\pi i k \omega} + a - 2}, \tag{13}$$
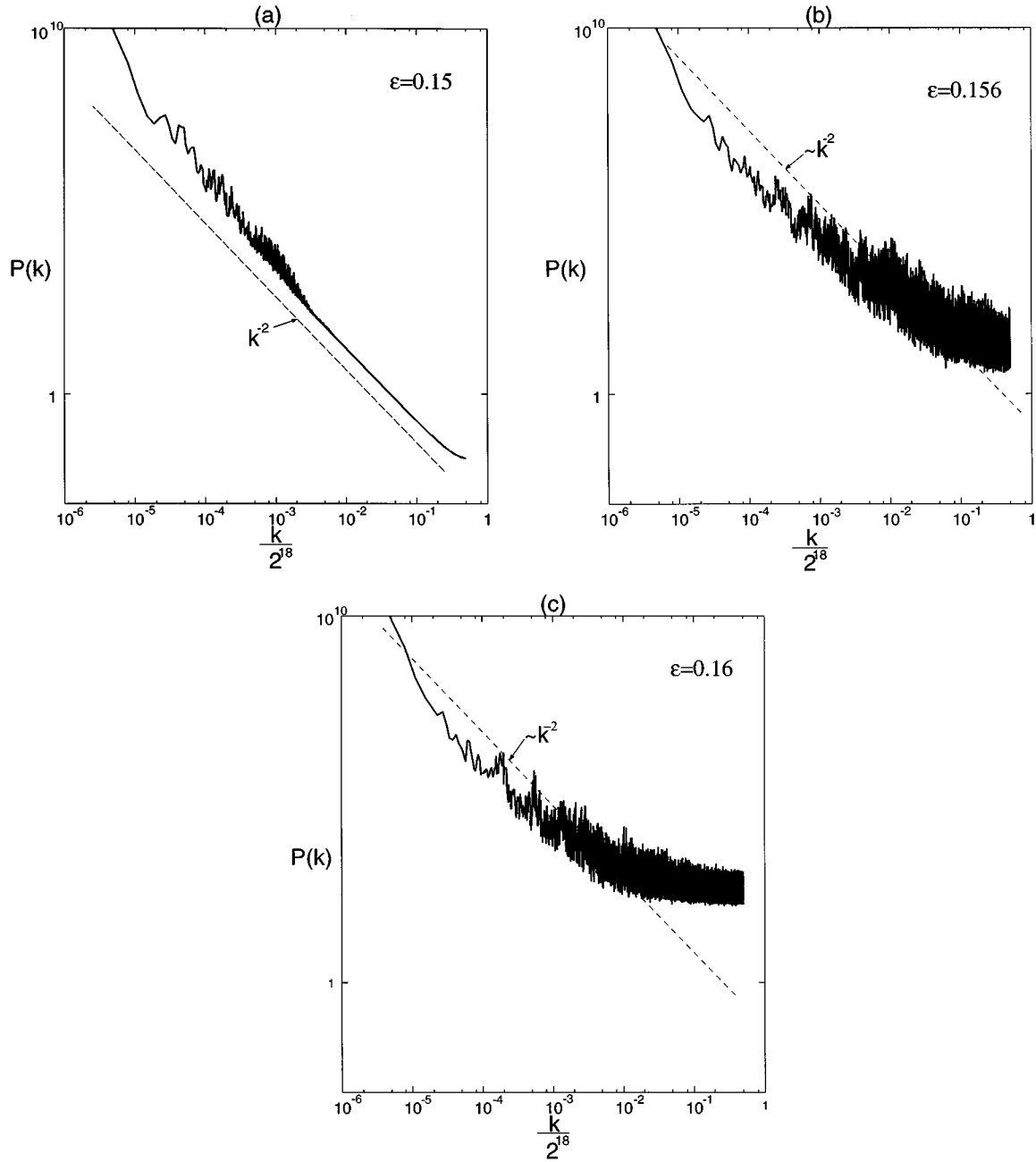
FIG. 10. Power spectrum $P(k) = |\hat{X}(k)|^2$ for $a = 3.0$ and (a) $\varepsilon = 0.15$, (b) $\varepsilon = 0.156$, and (c) $\varepsilon = 0.16$ obtained by averaging 100 different phase shifts θ_0 (shift of lattice points within the range of $1/F_k$). ($F_k = 317\,811$ and $2^N = 2^{18} = 262\,144$.)

$$\hat{X}(0) = \hat{X}_0(0) + \varepsilon^2 \hat{X}_2(0) + \varepsilon^4 \hat{X}_4(0) + \cdots, \qquad (14)$$

$$\hat{X}(\pm 1) = \varepsilon \hat{X}_1(\pm 1) + \varepsilon^3 \hat{X}_3(\pm 1) + \varepsilon^5 \hat{X}_5(\pm 1) + \cdots, \qquad (15)$$

$$\hat{X}(\pm 2) = \varepsilon^2 \hat{X}_2(\pm 2) + \varepsilon^4 \hat{X}_4(\pm 2) + \cdots, \qquad (16)$$

$$\vdots$$

$$X(\theta) = \hat{X}_0(0) + \varepsilon\{\hat{X}_1(1)e^{2\pi i \theta} + \hat{X}_1(-1)e^{-2\pi i \theta}\} + \varepsilon^2\{\hat{X}_2(0)$$
$$+ \hat{X}_2(2)e^{4\pi i \theta} + \hat{X}_2(-2)e^{-4\pi i \theta}\} + \varepsilon^3\{\hat{X}_3(1)e^{2\pi i \theta}$$
$$+ \hat{X}_3(-1)e^{-2\pi i \theta} + \hat{X}_3(3)e^{6\pi i \theta} + \hat{X}_3(-3)e^{-6\pi i \theta}\}$$
$$+ \cdots. \qquad (17)$$

When ε is gradually increased from zero, the terms of higher-frequency modes become larger in order. This explains the amplification of the torus oscillation for larger ε, as well as the slower decay of the Fourier coefficient with the wave number.

We have numerically calculated the power spectrum $P(k) = |\hat{X}(k)|^2$ for the three types of attractors, by using the largest 2^N points possible out of F_k points of the attractor of the functional map (1). The power spectra $P(k)$ are plotted in Fig. 10 for $a = 3.0$ and $\varepsilon = 0.15, 0.156, 0.16$, where $F_k = 317\,811$ and $2^N = 2^{18} = 262\,144$.

When the invariant curve is fractal, the first derivative of the Fourier series (6) is expected to lose its convergence. Indeed, the spectra $P(k)$ decrease with k slowly for the fractal torus. The maximum of the envelope of $P(k)$ decays

slower than k^{-2}, which means that $\hat{X}(k)\sim k^{-\alpha}$, where $0<\alpha<1$. The fractal nature is seen in the power spectra. For a smooth torus the spectra decay faster than or equal to k^{-2}.

It is interesting to note the analogy with the cascade process in turbulence. Equation (8) has a form similar to the Fourier expansion of the Navier-Stokes equation as regarding the formation of the cascade process by the term $\hat{X}(k)\hat{X}(k-k')$. In the case of fluid turbulence, this term brings about Kolmogorov's energy cascade. In contrast to the time dependence in turbulence, the Fourier modes of our functional equation fall into time-independent values at the fractal-torus regime. In fluid turbulence, the intermittency leads to sporadicalness in the vortex cascade, which brings about the deviation from Kolmogorov's 5/3 law. In our problem this corresponds to the sporadicalness of the extremal points. The degree of the sporadicalness changes with the parameter ε, as in the intermittency effect in turbulence, while the sporadicalness is lost at the the onset of chaos in the cascade of the functional equation. It will be interesting to search for a quantity in our problem corresponding to the energy cascade in turbulence.

IV. FRACTAL TORUS VERSUS SMOOTH TORUS

Let us reconsider the difference between smooth and fractal tori from a dynamical system viewpoint. Of course, the largest difference between the two types of tori is the length. The length of the fractal torus is infinite, in contrast to the smooth torus. This also leads to a difference in the orbital instability for the dynamics of the two types of tori. Smooth and fractal tori are both stable against the perturbation in the x direction. Although no exponential divergence of orbits exists for both, they are different from each other in terms of the phase sensitivity. Pikovsky and Feudel [4] have shown that two points on the SNA with close θ values separate from each other by introducing the following phase sensitivity exponent: For this, note that the absolute value of the first derivative of the orbit $|\partial x_n/\partial\theta_n|$ fluctuates with time and sometimes has a large burst. An arbitrarily large burst can appear when the map is iterated for infinite time steps. By differentiating Eq. (1) with respect to θ, one obtains

$$\frac{\partial x_{n+1}}{\partial\theta}=f'(x_n)\frac{\partial x_n}{\partial\theta}+\varepsilon g'(\theta). \tag{18}$$

Using this equation, one can compute the evolution of $\partial x_n/\partial\theta$ starting from some initial point (x_0,θ_0) and $\partial x_0/\partial\theta=0$. The phase sensitivity of Pikovsky and Feudel, then, is defined as

$$\Gamma_N=\min_{x_0,\theta_0}\max_{0\leq n\leq N}\left|\frac{\partial x_n}{\partial\theta}\right|.$$

This quantity must grow infinitely for a SNA with some power (and exponentially for a chaotic attractor) [4]. In our example, this quantity increases with power 2.5–3 for a fractal region, as it is shown in Fig. 11(a). At the pre-fractal-torus regime the quantity increases up to 10^6 steps (which
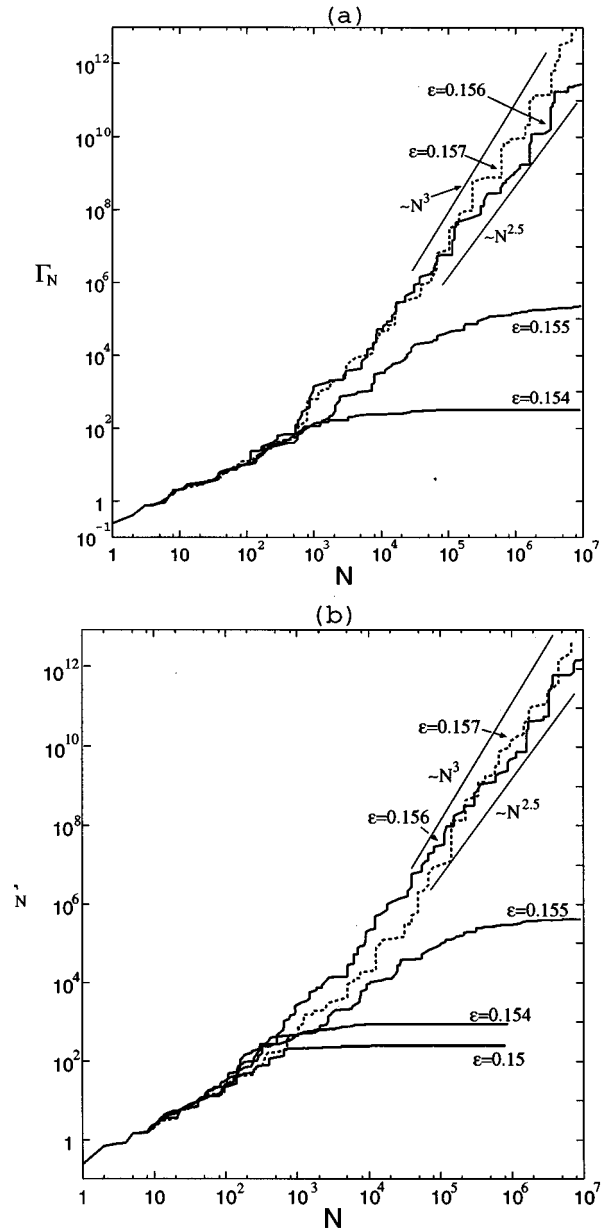

FIG. 11. (a) Γ_N and (b) $\Gamma_N^{(\varepsilon)}$ obtained for $a=3.0$ and $\omega=(\sqrt{5}-1)/2$. We have chosen 100 initial points (x_0,θ_0) randomly and iterated Eqs. (18) and (19) for each initial point, starting from $\partial x_0/\partial\theta=0$. Γ_N and $\Gamma_N^{(\varepsilon)}$ are obtained as the minimum of these 100 trajectories.

corresponds to the mesh scale of 10^{-6}) and then saturates, as is consistent with the results of the length in Sec. II obtained from the functional equation.

This Γ_N corresponds to the largest derivative of the attractor $X(\theta)$ of the functional map (3) for the mesh size about $N\times$(number of samples for $\min_{x_0,\theta_0}$). The larger the iteration number N, the larger the length of the attractor at the mesh.

The second difference between smooth and fractal tori lies in the parameter dependence of our invariant curve. For a fractal torus, there is sensitivity of the curve to the parameter ε at least for some value of θ. To confirm the sensitivity, we introduce the parameter sensitivity in the same way as
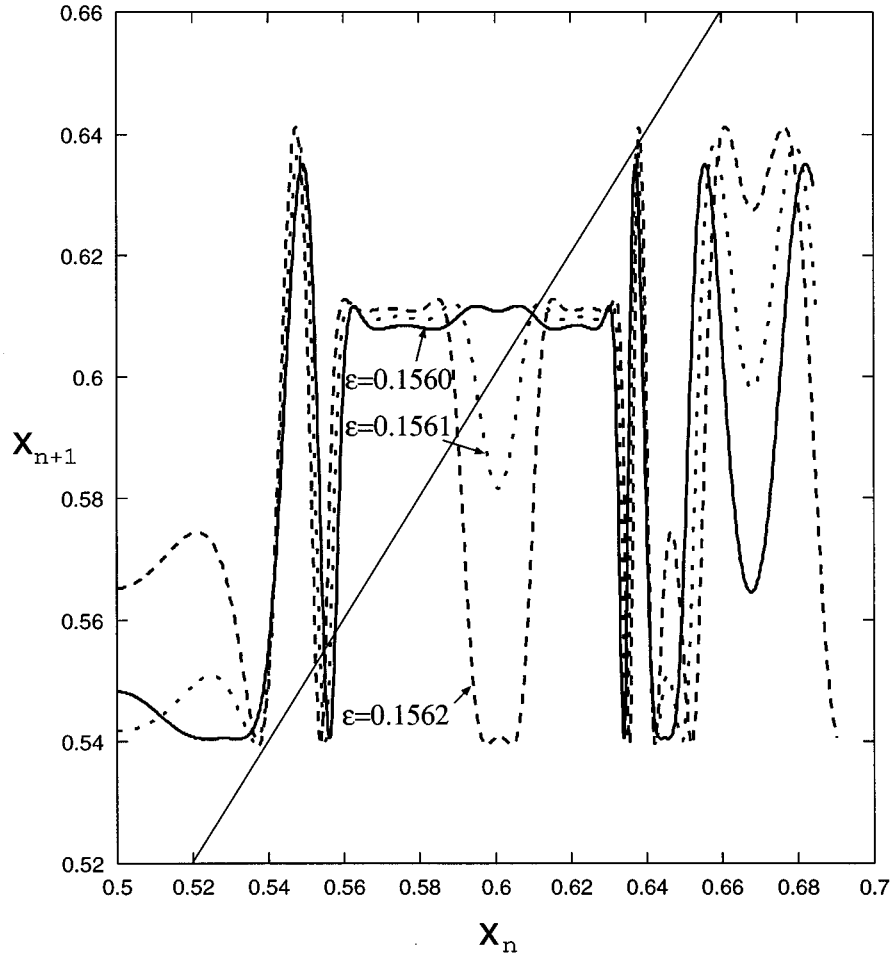
FIG. 12. Graph of the F_k map for $F_k = 55$ and $\theta_0 = 0$.

Γ_N [4]: By differentiating the first equation of (1) with respect to ε, we obtain

$$\frac{\partial x_{n+1}}{\partial \varepsilon} = f'(x_n)\frac{\partial x_n}{\partial \varepsilon} + g(\theta). \tag{19}$$

Then we define

$$\Gamma_N^{(\varepsilon)} = \min_{x_0,\theta_0} \max_{0 \leqslant n \leqslant N} \left| \frac{\partial x_n}{\partial \varepsilon} \right|.$$

In Fig. 11(b) we have plotted this parameter sensitivity. Again this quantity grows with some power for the fractal torus. In our model this power is identical to that for Γ_N, i.e., the power 2.5–3 [see Fig. 11(b)]. This is expected since Eq. (18) for $\Gamma_N^{(\varepsilon)}$ has the same form as Γ_N [Eq. (19)], except that the last term is smooth. The power-law increase of $\Gamma_N^{(\varepsilon)}$ implies that the fractal torus always has this kind of parameter sensitivity.

Such parameter dependence is also reflected in the Lyapunov exponent of each attractor. The sensitivity of the Lyapunov exponent to the parameter ε is relatively sharp in the region of the fractal torus, while the parameter dependence is smooth in the region of normal torus, as we have mentioned earlier.

The third difference lies in the loss of convergence in the derivative of $X(\theta)$ for the fractal torus. Indeed, the Fourier expansion of $X(\theta)$ decays faster than or equal to $1/k$ for a smooth torus, while for the fractal one, it decays slower than $1/k$, as discussed in Sec. III in terms of $P(k)$.

This loss of convergence corresponds to the power spectrum of the time series of x_n since the relation $\theta = \omega n + \text{const}(\text{mod}1)$ leads to a direct correspondence between θ and time. It is shown in [5] that the power spectrum of the time series is singular for SNAs. There the number of singular points whose power is larger than a threshold decreases with some power with the threshold, while it decays exponentially for a smooth torus. This characteristic is another manifestation of the loss of convergence in the Fourier modes of the derivative.

The question remains what causes the transition from a smooth to a fractal torus. One possible route to the SNA is the crisis between stable and unstable invariant curves [7]. In our model, however, the unstable torus (continued from the unstable fixed point of the logistic map) lies far away from the stable one and has nothing to do with the fractalization. Hence there must be another possible mechanism for the emergence of SNAs. In the functional equation, this can be seen in the loss of convergence in the Fourier series. How is the loss of smoothness expressed in terms of dynamical systems for the original two-dimensional map?
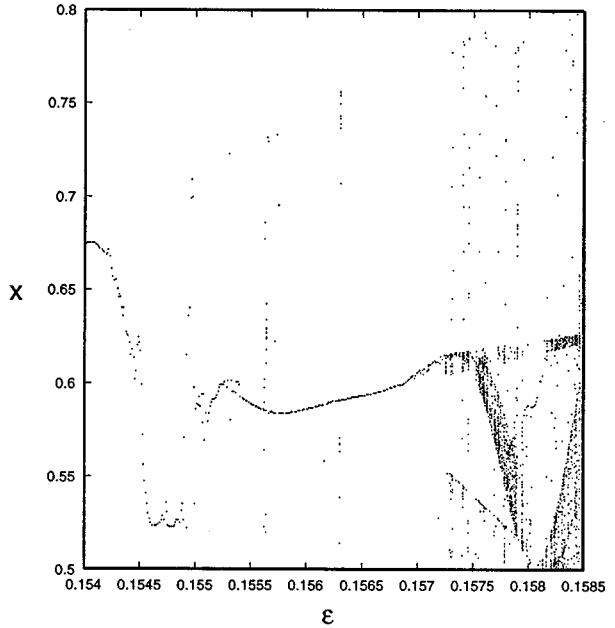
FIG. 13. Bifurcation diagram obtained from the F_k map for $F_k = 987$. A sequence of x_n generated by the F_k map is plotted over 100 steps after 2900 points are discarded. The time series is plotted for each ε value. The initial condition for the next ε value is chosen from the orbit x_n for the previous ε, while ε is incremented by 0.0001 between 0.154 and 0.1585.

To study this problem, we have introduced the following F_k map. If we approximate ω by F_{k-1}/F_k and start iterations from any point (x_0, θ_0), the orbit will be periodic in θ with period F_k. $[\theta_{F_k} = \theta_0 + F_k \omega = \theta_0 + F_{k-1} = \theta_0 (\mathrm{mod}\, 1).]$ Thus a composition one-dimensional map is constructed as the F_k-times iterations of the original two-dimensional map. Let us call this composition map an F_k map. The F_k map is a function of x if we fix the initial θ_0. The shape of the graph of the F_k map depends on the initial θ_0, ε, and k. Figure 12 gives a sequence of examples of the F_k map. The map converges to the functional map as k goes to infinity. We can infer the behavior of the functional map from the F_k map.

In Fig. 13 we have plotted the bifurcation diagram of the F_k map by taking $F_k = 987$. (This rather small value of F_k is chosen so that the characteristic feature of the one-dimensional map is visible.) Since the onset of the fractal torus and chaos can slightly differ between $\omega_k = F_{k-1}/F_k$ and $\omega = (\sqrt{5} - 1)/2$, we have to take into account the possible shift of the bifurcation parameter to compare the result of the F_k map with that of the functional map.

Let us look at the SNA region ($0.1542 \leqslant \varepsilon \leqslant 0.1573$) in Fig. 13. First, we can see a sensitive dependence on ε, as we have discussed earlier. Second, we can see some points where the map does not approach a fixed point and instead shows chaotic behavior. By the definition of a SNA, the F_k map must have a fixed point when k goes to infinity. When ω is approximated by a rational (say, by F_{k-1}/F_k with $F_k = 987$), this does not have to be true. It seems that there always exists at least one chaotic point for some initial θ_0 at every value of ε in the SNA region. From this result we

propose the following picture of a SNA viewed from the F_k map. In the SNA region, the F_k map has dense ε values leading to chaotic behavior for some θ_0, whose measure goes to zero with the increase of the mesh size F_k. This kind of ''partially chaotic'' behavior may be related to the existence of a positive local Lyapunov exponent discussed by Pikovsky and Feudel [4].

We also note that the F_k map has a strong sensitivity to θ_0 for the SNA. A change of $F_k(x; \theta_0)$ with θ_0 becomes faster as k goes to infinity. This feature of the F_k map is consistent with the fractal nature of the torus.

V. FROM A FRACTAL TORUS TO CHAOS

What characterizes the transition from a fractal torus to chaos? First, it is clear that the functional map (3) loses its convergence. This is interpreted as the loss of stability of the fixed point in the functional space. The functional map shows chaotic dynamics (possibly having a high-dimensional attractor) there, although the snapshot pattern of $X_n(\theta)$ remains fractal with the power 0.88–1. Beyond the onset of chaos, the chaotic fluctuation of $|X_{n+1}(\theta) - X_n(\theta)|^2$ increases with ε. It is interesting to study the transition from a fixed point to chaos in the functional space as a high-dimensional dynamical system. As for the bifurcation to chaos, this transition might be referred to as intermittent chaos in the functional space.

To verify this idea we have again considered the F_k map, the composite one-dimensional map, given in Fig. 12. From the graph a kind of intermittent transition is seen at about $\varepsilon \sim 0.1561$. Indeed there is a tangent bifurcation from the fixed point, by which the attractor of the F_k map changes to a chaotic one. This dependence on ε does not change qualitatively with k, if k is large enough. Then the intermittent character of the transition from a fractal torus to chaos in the functional map is inferred by taking the limit $k \to \infty$.

As k is increased, the sensitivity on ε will be sharper, not only for a fractal torus but also for a chaotic attractor. The sensitivity of the shape of the graph leads to sensitivity of the Lyapunov exponent. This gives an explanation of the sensitive dependence of the Lyapunov exponent on ε, previously mentioned.

VI. SUMMARY AND DISCUSSION

We have verified the existence of the SNA in our quasi-periodically forced logistic map by measuring the Lyapunov exponent and the length and the number of extrema of the attractor and power spectra. We have found that the SNA exists in a finite interval in the parameter space and concluded that the SNA is no other than the fractalization of the torus in [2]. It should be noted that Anishchenko *et al.* [8] have also recently discussed the fractalization of a torus to chaos as a SNA by using a forced circle map.

To understand the mechanism of fractalization and transition to chaos, we have introduced a *functional map (functional equation)*. The attractor of the two-dimensional map is represented as a fixed point of the functional map in the functional space. From this viewpoint, fractalization of the torus is expressed as the change of the fixed point solution of the functional map, from a smooth to a nonsmooth one. The

transition to chaos might be regarded as an intermittent chaos in the functional space.

We have also introduced the F_k map, a composition of the map over F_k steps. This F_k map is a kind of cross section of the functional map. With this map, the origin of the fractalization of the torus is related to the sensitive dependence on the initial phase θ_0, while the transition to chaos is associated with the intermittency from the fixed point in this F_k map.

There has been a general interest in the search for a different type of dynamics in a forced system [11], as it has been pioneered by Moser [12]. There the instability arising from the off-diagonal element [13] in the Jacobi matrix may lead to a different dynamical behavior. Such instability is also seen in the convective instability in the open flow problem [14], where the instability due to the off-diagonal element leads to a rich variety of dynamics [15]. The strange nonchaotic attractor in our model is also due to the instability by the off-diagonal element, as it is characterized by the phase sensitivity of the amplitude. It is interesting to explore dynamical systems with such a type of instability in general, where the present functional map method may be useful.

The study of the functional equation itself is an interesting topic. In particular, the attractor of the functional map is high-dimensional chaos, when the fractal torus is replaced by chaos. The one-dimensional string $X(\theta)$ is spatially fractal and temporally chaotic, as in the problem of developed turbulence. In this sense, the model may provide a different class of spatiotemporal chaos. Indeed, the functional equation can be viewed as a coupled map with a long-range coupling, by which each lattice point is coupled with the point at a distance of F_{k-1} sites.

It may be interesting to note an analogy between our functional equation and the so-called Weierstrass function. The Weierstrass function is defined as

$$W(\theta) = \sum_{n=0}^{\infty} a^n \cos b^n \pi \theta \quad (ab \geq 1, \quad 0 < a < 1). \quad (20)$$

The topological dimension of the Weierstrass function is one, but its fractal dimension is believed to be more than one. The Fourier coefficient of $W(\theta)$ decreases as $k^{-1 + \ln(ab)/\ln b}$ with the wave number k. As Yamaguchi and Hata [16] have demonstrated, the fractal nature of Weierstrass (and Takagi) functions are derived from the functional equation. Unfortunately, their analysis is not applicable to ours since their functional equation is linear in contrast to ours. Still some analytical studies on the functional equation as well as the renormalization-group analysis [17] for the perturbation series (10) should be of importance in the future.

ACKNOWLEDGMENTS

[1] K. Kaneko, *Collapse of Tori and Genesis of Chaos in Dissipative Systems* (World Scientific, Singapore, 1986).

[2] K. Kaneko, Prog. Theor. Phys. **71**, 1112 (1984).

[3] C. Grebogi, E. Ott, S. Pelikan, and J. A. Yorke, Physica D **13**, 261 (1984).

[4] A. S. Pikovsky and U. Feudel, CHAOS **5**, 253 (1995).

[5] F. J. Romeiras, A. Bondeson, E. Ott, T. M. Antonsen, Jr., and C. Grebogi, Physica D **26**, 277 (1987).

[6] U. Feudel, J. Kurths, and A. S. Pikovsky, Physica D **88**, 176 (1995).

[7] J. F. Heagy and S. M. Hammel, Physica D **70**, 140 (1994).

[8] V. S. Anishchenko, T. E. Vadivasova, and O. Sosnovtseva, Phys. Rev. E **53**, 4451 (1996).

[9] M. Ding, C. Grebogi, and E. Ott, Phys. Rev. A **39**, 2593 (1989).

[10] Y. Lai, Phys. Rev. E **53**, 57 (1996).

[11] O. E. Roessler, C. Knudsen, J. L. Hudson, and I. Tsuda, Int. J. Intell. Syst. **10**, 15 (1995).

[12] J. Moser, J. Diff. Equations **5**, 411 (1969).

[13] M. Courbage and D. Hamdan, Phys. Rev. Lett. **26**, 5166 (1995).

[14] R. J. Deissler and K. Kaneko, Phys. Lett. A **119**, 397 (1987).

[15] F. H. Willeboordse and K. Kaneko, Physica D **86**, 428 (1995), and references cited therein.

[16] M. Yamaguti and M. Hata, Hokkaido J. Math. **12**, 333 (1983).

[17] S. P. Kuznetsov, A. S. Pikovsky, and U. Feudel, Phys. Rev. E **51**, 1629 (1995).